THERMAL FATIGUE OF METALS

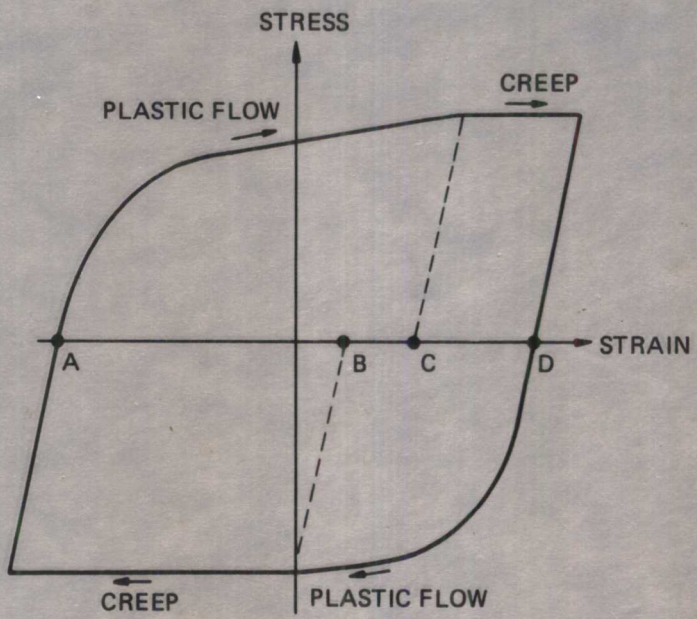

ANDRZEJ WEROŃSKI
TADEUSZ HEJWOWSKI

THERMAL FATIGUE OF METALS

ANDRZEJ WEROŃSKI
TADEUSZ HEJWOWSKI
Technical University of Lublin
Lublin, Poland

Marcel Dekker, Inc. New York • Basel • Hong Kong

Library of Congress Cataloging-in-Publication Data

Weroński, Andrzej
Thermal fatigue of metals / Andrzej Weroński, Tadeusz Hejwowski
p. cm. -- (Mechanical engineering; 74)
Includes bibliographical references and index.
ISBN 0-8247-7726-3 (acid-free paper)
1. Metals--Thermal fatigue. 2. Thermal stresses. I. Hejwowski, Tadeusz. II. Title. III. Series: Mechanical engineering (Marcel Dekker, Inc.); 74.
TA460.W46 1991
620.1'61--dc20 91-20558
CIP

This book is printed on acid-free paper.

Marcel Dekker, Inc.
270 Madison Avenue, New York, New York 10016

Current printing (last digit):
10 9 8 7 6 5 4 3 2 1

PRINTED IN THE UNITED STATES OF AMERICA

Preface

Systematic investigation into the nature of thermal fatigue began in the early 1950s, the impetus coming principally from the continually increasing working temperatures employed in industry and a growing need for greater efficiency and reliability. The commonly accepted definition of thermal fatigue is that it is a complex of phenomena appearing in material exposed to cyclically varying temperatures in the presence or absence of external load. The process of thermal fatigue of a particular component is usually considered in association with mechanical fatigue, creep, corrosion, and similar factors. These phenomena undoubtedly contribute to the failure, as thermal cycling causes alternating strains to occur and the average temperature of the cycle is usually high enough for both corrosion and creep to become significant factors. All these topics have been studied extensively by researchers, but unfortunately, attempts to approximate thermal fatigue by considering each of these phenomena in isolation, then summing up the damages introduced, usually produce erroneous results.

The next difficulty encountered is that in considering thermal fatigue in practice, the exact form of the loading cycle of a particular component is very rarely known—what we know, in fact, is the approximate range of thermal variations at its surface. These should, in turn, be translated into thermal variations below the surface and thermal stresses and strains there. Usually, considerable experimental effort is needed to obtain true temperature profiles. Calculations of thermal stresses and strains require detailed knowledge of material properties, and these change with an increasing number of cycles and can be only roughly approximated.

This book brings together applied and analytical aspects of these phenomena. Attention is focused on the practical aspects and the book is devoted to both experimentalists who interpret and generate thermal fatigue data and users whose principal concern is to find a remedy to thermal fatigue problems. Accordingly, the book is intended to serve for both instruction and reference.

This book consists of separate chapters on mechanical fatigue, creep, heat-resistant materials, and thermal fatigue. The phenomena are presented in the order in which they attracted the notice of technicians. The advantage of this sequence is

that we approach thermal fatigue gradually, meeting en route phenomena some or all of which are always present in any practical case in which thermal fatigue might occur. Also shown in the book is how to make practical use of the information provided on thermal fatigue. The example utilized is that of a mold for centrifugal casting working under extreme thermal conditions. The following steps are taken to mitigate the effects of thermal fatigue:

Defining the problem
Specifying the working conditions
Designing a test procedure to simulate the crucial factors
Running tests to determine the effect of thermal cycles on material and to rank the candidate materials
Finally, improving the mold design

Thermal fatigue arises in a greater variety of situations than can be discussed in detail herein. The wide domain in which thermal fatigue may make a significant or total contribution to failure has three boundaries:

1. The area in which mechanical stress cycling is severe and thermal stressing is moderate
2. The thermal shock region, in which temperature change and rate of change is so great that failure occurs within one or a very few cycles
3. The region of creep failure, characterized by constant mechanical loading and relatively high temperatures during very long thermal cycles

Within these bounds there are situations normally understood as thermal fatigue. The discussion covers:

1. End products subject to thermal fatigue in operation: for example, internal combustion engines, where the benefits of thermal fatigue design and manufacture appear as increased reliability and efficiency
2. Manufacturing tools subject to thermal fatigue, which must be minimized in the interest of production costs. The tools considered include ingot molds, equipment for heat treatment, mill rolls, and forging equipment.

Chapter 8, the heart of the book, comprises a discussion of thermal fatigue in particular industrial components in reference to their working conditions. Examples are provided of a variety of machinery in which thermal fatigue problems are common and must be overcome. This book was written to assist in satisfying that imperative of modern engineering.

We wish to express our gratitude to the authors and publishers who kindly granted us permissions to cite their works, but first of all we would like to thank George Munns, who read most of the manuscript and made many helpful comments.

Andrzej Weroński
Tadeusz Hejwowski

Contents

1

Mechanical Fatigue

1.1 INTRODUCTION

The commonly accepted definition of mechanical fatigue is that it is a complex of phenomena caused by progressive, cumulatively increasing damage to material accumulated in each of successive loading cycles. It is noteworthy that fracture is produced by stresses that are only a fraction of the static strength and that the number of loading cycles encountered in service by an element can be as high as 10^8. Some authorities maintain that about 80 to 90% of all failures ending in fracture are connected with fatigue. Fatigue failure caused by material imperfections is rather rare; the majority of accidents have, as a sole or contributory cause, a design or maintenance fault. Since Wöhler's investigation of the causes of a series of catastrophic failures to railway axles, summarized in his 1870 article, scores of thousands of publications devoted to mechanical fatigue have been published, but the knowledge gathered has been neither cohesive nor comprehensive. Furthermore, it seems unrealistic to reach a converse opinion when considering the variety of factors that influence the fatigue life and the difficulties in describing the state of real solid matter.

Mechanical fatigue is a particular case of thermal fatigue. Both have the same source of damage: repeatedly applied stresses of different origin, caused by either external load or temperature transients. This intuitively deducted identity is only sometimes found to be valid; its particular aspects are discussed later. In many situations encountered in industry, a device such as a forging die is loaded simultaneously by external forces and thermal stresses. Moreover, to discuss thermal fatigue it is convenient to accept the descriptive methods developed in earlier studies.

The process of fatigue failure can be divided into the following successive stages:

Formation of a microcrack nucleus
Propagation (growth) of the fatigue crack
Final rupture

These three stages are discussed in separate sections of this chapter.

1.2 FATIGUE TESTS

Any attempt to create a model of crack nucleation must be well supported by experimental data, and therefore some findings should be obtained first. Mechanical fatigue experiments are carried out in a range of temperatures from almost absolute zero to approaching the melting point of the specimen, in various media, often in vacuum or laboratory air and with a coexisting factor such as exposure to neutron flux while loading with fluctuating force. Despite these differences, all such experiments can be classified as follows:

1. Those in which the external cyclic or fluctuating load amplitude is held constant throughout the entire test run, whether by bending, push-pull, torsion, rotating cantilever, or a more "sophisticated" method. Such a setup is called *load controlled.* An example is the classical experiment of Wöhler.
2. Those in which the amplitude of load is not a crucial factor and thus is allowed to change during the test. Interest focuses solely on the strain amplitude. Experiments in this group are called *strain controlled.* The method is realized in practice by attaching a suitable extensometer to the specimen to measure deformation and using it as a controlling device. During testing the stress amplitude is allowed to vary while the strain amplitude is held constant.

Thermal stresses are usually strain controlled; for example, an ingot mold wall is exposed to thermal shock when poured with molten metal but is restrained from deformation by cooler portions of the wall material. By analogy, pressure loads are usually load controlled. Between these two extremes are a vast number of real loading situations that are mixed and more complicated in nature.

The external load is usually applied repeatedly with a chosen frequency while maintaining constant conditions. However, in a few situations a random variety of loads are utilized: to study the response of carriage springs, for example. This load spectrum can either be recorded during use of the device and reproduced in laboratory tests, or can be generated by a suitable device, usually a computer.

The load spectrum is characterized by the following quantities:

Medium stress, the arithmetic mean of maximal and minimal stresses in the cycle $[\sigma_{av} = (\sigma_{min} + \sigma_{max})/2]$

Stress amplitude, half the difference between the maximal and minimal values of stress in the cycle

Stress ratio, the ratio of maximal value to minimal value of stress in the cycle $(R = \sigma_{max}/\sigma_{min})$

The information concerning loading conditions becomes complete on specifying the cycle shape. Both cycle shape and frequency of cyclic loading are especially important in tests carried out at elevated temperature or in aggressive media.

The results obtained in the load-controlled tests are usually plotted in terms of the stress versus the logarithm of the number of stress cycles imposed. A batch of

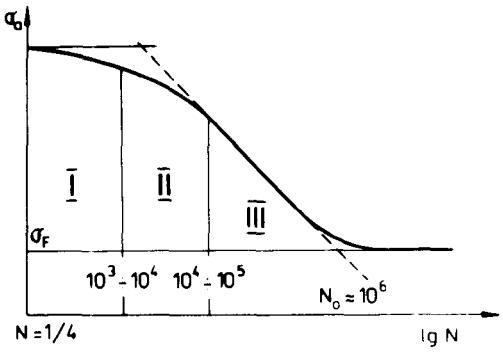

Figure 1.1 Diagram of Wöhler plot.

identical specimens is tested in practice under the same conditions, and the average number of stress cycles withstood is treated together with the cycle amplitude as coordinates of the point displayed in the plot. It is worth noting that the results obtained within one batch of specimens can differ by as much as one order of magnitude (e.g., Yokobori, 1954), and the curve drawn to represent the entire set of results is, in fact, the curve of best fit. A plot made in such a way is commonly referred to as a *Wöhler plot*. The leftmost point on the plot (see Fig. 1.1) corresponds to one quarter of the cycle and is usually in reasonable accord with the results of a static tensile test. As shown, the curve can be approximated by three dashed-line segments. Hück (1981) published a procedure to calculate the inclination of the middle segment and the limiting magnitude of stress, below which the indefinite life of the tested specimen is expected, being the ordinate of the rightmost segment and called the *fatigue strength* or *fatigue limit*. This procedure was developed on the basis of statistical considerations, over 600 Wöhler plots appearing in the literature having been taken into account for this purpose. The input data are the static strength or hardness, yield strength, quantities characterizing the size and shape of the specimen, cyclic stressing conditions, and the thermal treatment given to the specimen. Of course, such a description of the Wöhler plot is only approximate—to be used until experimental data regarding the material in question are provided. The portion of the plot (Fig. 1.1) marked "I" is called a *quasi-static range*, as the elongations of fatigued specimens reached just before the fracture are comparable with those found in static tests. Area II represents *low-cycle fatigue*, and at such stress amplitudes, yielding cannot be neglected, plastic deformation being a substantial part of the total strain range. The stress amplitudes and corresponding numbers of cycles relating to yielding that is restricted to the zone just ahead of the crack tip constitute region III, called a *high-cycle fatigue region*.

The presence of elastoplastic deformations causes hysteresis loops to appear in a plot of stress imposed on the specimen versus resultant strain (see Fig. 1.2). The area encircled by the loop is a measure of the energy supplied to the specimen.

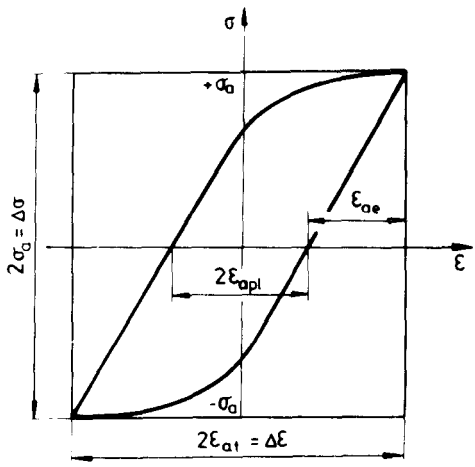

Figure 1.2 Hysteresis loop. σ_a, amplitude of cyclic stress; ε_{ae}, amplitude of elastic strain; ε_{apl}, amplitude of plastic strain; ε_{at}, total strain amplitude.

Hysteresis loops can be recorded in both strain- and load-controlled experiments. The experimental data obtained show that the hysteresis loop usually changes during early stress cycles to stabilize before one-third to one-half of the fatigue life is spent and achieves a saturation state characterized by constant values of stress amplitude or strain. The termination of fatigue life is accompanied by a loss of stability. The behavior of materials under test is illustrated schematically in Fig. 1.3. The upper curves were obtained in strain-controlled experiments, the lower ones in load-controlled experiments. The instances shown in Fig. 1.3a and d are referred to as *cyclic hardening*, those in Fig. 1.3b and e as *cyclic softening*, specimens c and f having revealed stability.

It should be stressed, however, that under more severe conditions (e.g., at slightly elevated temperatures), a stable hysteresis loop cannot be observed at all. Investigating the cyclic response of AISI 316 stainless steel, Jaske and Frey (1982) found that the saturation state was achieved in room-temperature tests and that a small alteration in test temperature (i.e., to 427 K) resulted in an ever-changing hysteresis loop up to 10^5 cycles.

The following relationship, determined experimentally by Manson (1953) and Coffin (1954), is an alternative way of describing the fatigue process:

$$N_f^K \Delta\varepsilon_{pl} = C$$

where

N_f = number of stress cycles to fracture
$\Delta\varepsilon_{pl}$ = plastic strain range
K, C = coefficents dependent on specimen material and test conditions

In the double-logarithmic coordinate system the plot of the foregoing equation is a straight line, the slope of which is defined by a K coefficient ranging from 0.4 to 0.8 but generally near 0.5. The C coefficient is usually found from the ultimate strain in the tensile test ($N_f = \frac{1}{4}$). Moreover, what is especially interesting, the relationship was proved valid in thermal fatigue tests. Attempts to replace the thermal fatigue test by a general fatigue tests, which provides a thermal strain range by imposing sufficiently large stress amplitudes, are of limited validity. In many instances even an application of stresses at the upper temperature of the thermal cycle provided very optimistic results—longer specimen endurance times than those obtained in a thermal fatigue test (e.g., Coffin, 1958).

The extent of the cyclic hardening increases with the stacking fault energy. The hypotheses explaining this phenomenon grew on the basis of dislocation considerations, formerly restricted to static tests. The hypothesis of Feltner (1965) explaining cyclic hardening applies to face-centered cubic (fcc) metals. It involves the creation of dislocation loops as a feature of cyclic hardening and the forcing of screw dislocations to circumvent the debris obstacles by cross-slip, which results in the formation of additional dislocation loops. In the saturation state, the number of dislocation loops remains constant, with the loops performing flip-flop motions between the two stable locations, enabling the reversibility of cyclic deformations.

High-cycle fatigue is relatively poorly explored. Tests on steels are usually terminated at about 10^6 cycles; continuation is very time consuming and expensive. It compels us to apply higher cycle frequencies, which in turn creates problems in maintaining constant ranges of stress or strains. For that reason, the fatigue strength is related to the number of cycles defined, usually being 1×10^6 for steels and only

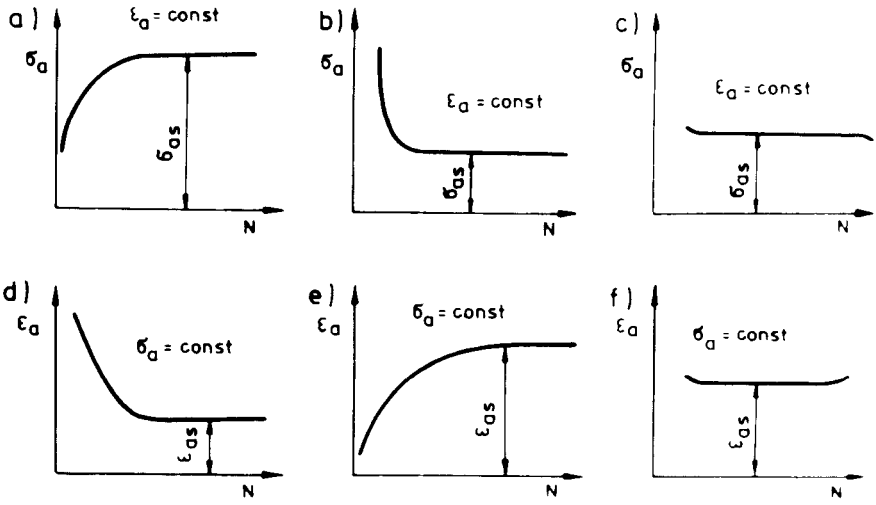

Figure 1.3 Behavior of various materials in fatigue tests in strain (a–c) and in load-controlled (d–f) experiments. (From Kocańda, 1985.)

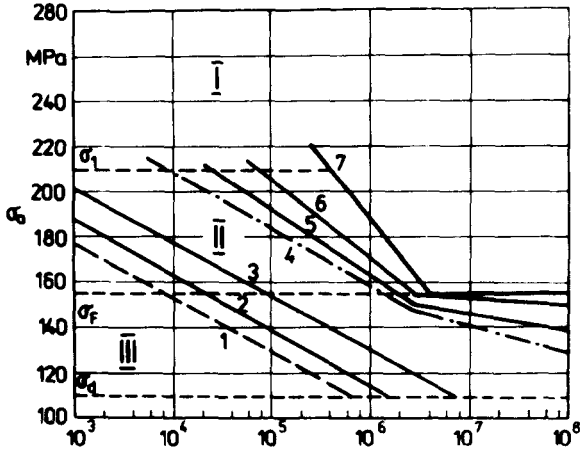

Figure 1.4 Wöhler plot for Armco iron.

exceptionally as high as 10^7 cycles. The value of the fatigue strength is found in tests involving reversed symmetrical cycles and more rarely, fluctuating cycles. The choice of cycle number limits is connected to the fact that in moderate test conditions, the knee of the *S/N* plot is observed below about 10^5 to 10^6, and the curve runs parallel to the axis of the abscissa. In more severe conditions, the horizontal portion of the plot can be absent altogether.

There are two possible design concepts:

1. A fail-safe design, in which the cyclic stresses occurring in the element are, by proper design, kept within the stress range that provides long life,
2. A design that assumes the existence of flaws in the applied component, and their gradual extension, described below.

1.3 MICRO- AND MACROSCOPIC PATTERNS OF FATIGUE

Investigations of fatigue failures almost invariably produce the same result: A fatigue crack nucleates at the surface of a loaded element and gradually grows to a critical length above which the crack is no longer stable, and propagates with subsonic velocity, causing final rupture of the element. This suggests that the state of the free surface of the element describes the damage accumulation within the fatigued element, and that changes in the microstructure found on the surface are crucial. Kocańda (1961a, b) investigated Armco iron in bending, interrupting the test several times to find the sequence of microstructural changes accompanying the fatigue damage. The fatigue limit was 155 MPa, the yield strength was 210 MPa,

the amplitudes of stresses imposed on the specimens were in the range 80 to 240 MPa, and the corresponding numbers of cycles ranged from 10^3 to 10^8. Details of microstructural changes were studied on carbon replicas by means of transmission microscopy in addition to examination under a metallographic microscope. Figure 1.4 demonstrates a Wöhler plot (marked 7) obtained by experiment and the zones of characteristic microstructural changes. For stresses exceeding σ_1 (region I) the observed changes were very distinct, contrary to the very low stresses below σ_d, where the microstructure remained intact. In region III of stress amplitudes the microstructural changes, however, visible, did not lead to rupture, unlike the situation in region II. The inclined, numbered segments introduce a classification of the characteristic phases of fatigue.

1. In stress amplitude region I, distinct plastic deformation is observed after a few fatigue cycles. Narrow slip bands are present which are not grouped in any particular direction but rather, are randomly oriented to the acting stresses. Cracks are observed at the boundaries of heavily deformed grains and within slip bands. A rapid extension of cracks, passing grain boundaries, is observed between lines 6 and 7.
2. In region II, slip bands appear between lines 1 and 2, growing to form distinct bands between lines 2 and 3. Line 3 corresponds to blocking slip bands by grain boundaries. Between lines 4 and 5, slips induced in adjacent grains, when joined, constitute the microcrack nuclei clearly visible between lines 5 and 6; lines 6 and 7 mark the region of crack extension from an initial size of 0.1 to 0.5 mm until final rupture.
3. The pattern observed in region III is similar to the one described just above. The lower amplitude of acting stresses reduces the number of grains with developed slips and extends their incubation period. The microcracks revealed are blocked considerably longer on grain boundaries.

The pattern presented seems sketchy—the chemical composition of tested material enables precise interpretation of the phenomena observed, at the expense of oversimplification. As commercial alloys usually have a multiphasic structure, they are much more difficult to study, and the pattern would need to be broadly supplemented. Armco iron, which has a very low content of alloying additives, was shown to be sensitive to interstitials (e.g., N and C), which shift the Wöhler plot relative to coordinates, leaving the shape and pattern of changes intact. The presence of a fatigue limit is controlled by grain size, and for fine-grained steels is often observed. It therefore is interesting to note the experimental results obtained on commercial materials. For example, Maiya (1977) revealed short, one-grain-diameter-size (0.1 mm) cracks in stainless steel tested in air at 866 K in a low-cycle regime after 74 to 91% of fatigue endurance.

Irreversible microstructural changes, which threaten specimen integrity, appear in a very early stage of the fatigue proces. Thorough annealing, repeated after some number of cycles, may be efficient for a low-cycle situation when repeated after, say, 0.1% of fatigue endurance.

Nisitani and Takao (1981) investigated two grades of low-carbon steels (0.13 and 0.17 C): annealed α-brass and aged Al alloy. Bending tests were carried out at ambient temperature in air, and interrupted after a defined number of cycles in order to take replicas. It was found that in aged Al alloy, slip bands were confined to a small portion of the grain, the surrounding matrix remaining almost intact. In the course of fatigue progress, these bands developed and were transformed into a crack nucleus. In contrast, in the other materials the region of accumulating damage was far greater, reaching grain size. The repetition of stresses produced new slip lines, with the region of heavy slips subsequently transformed into a crack. It was also revealed that in low-carbon steels tested below the fatigue limit, microcrack nuclei were formed, but their slow growth was soon terminated.

The slips observed in Armco iron had a medium width of 100 lattice constants and the surface irregularity was on the order of 1000 lattice constants (Kocańda, 1961b). Slips proceed along definite crystallographic planes and axes. Two situations are frequently encountered: lamellar slips occurring in parallel planes and turbulent slips where mutually inclined slip planes are operating. The wavy appearance of slip lines points either to the presence of obstacles on the path of moving dislocations or to the presence of cross-slip. The latter is favored by a high value of staking fault energy. Microirregularities of the surface, even amounting to several micrometers, are products of slips and microcracks as well as of grain deformations. The pattern of extrusions and intrusions, rarely observed in its pure form, is depicted in Fig. 1.5. Extrusion is a squeezed-out flake of metal, the height of which is about 1 μm, and the neighboring extrusions are separated by 1 to 10 μm for copper. Intrusion, which does not necessarily accompany the former, is a fine crevice between extrusions. It is intuitively obvious that squeezing metal flakes out of the surface produces a void underneath. The risk of seizing up its walls by adhesion forces is reduced by the scale of the phenomena described (i.e., translation of relatively high volumes of material), and therefore it is a tempting entry point for crack nucleation hypotheses.

Lozinski and Romanov (1965) investigated commercial iron containing 0.03% C.

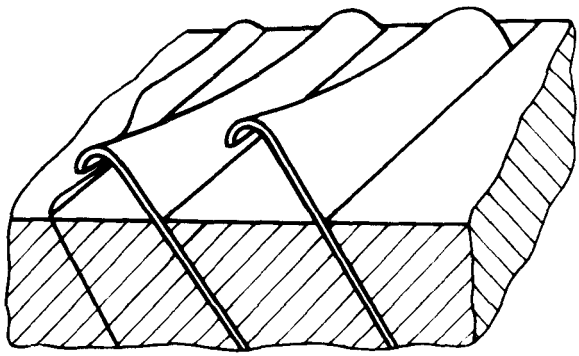

Figure 1.5 Pattern of extrusions and intrusions.

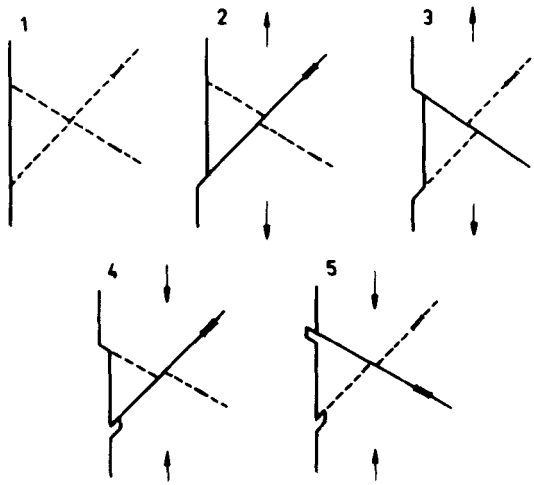

Figure 1.6 Sequence of slip movements producing extrusion and intrusion. (From Cottrell and Hall, 1957.)

Tests were done in high vacuum, with repeated bending, at temperatures of 293 to 1073 K. The sets of extrusions accompanied by intrusions were found only at elevated temperatures (above 573 K). The microrelief areas observed on the surface were often of complicated form, because in each grain (composed of subgrains) there is a set of various slip systems. The given test conditions favored some possibilities, rendering others negligible. An important achievement was the experimentally proved presence of voids below extrusions.

Cottrell and Hull (1957) proposed a model of extrusion and intrusion formation based on the coexistence of two slip systems and the sequence of slip motions (Fig. 1.6). It can be seen that the two intersecting slip systems are actuated in sequence and that during the tension half-cycle an intrusion is formed, as opposed to an extrusion during the compressive phase.

The model introduced by Mott (1958) is more independent of microstructure than that of Cottrell and Hall. In this model, extrusion results from the motion of a screw dislocation (the conservative and the cross-slip) having its extremities attached to the free surface, along the path $ABCD$, and the cavity lying underneath it, along $A'B'C'D'$ (Fig. 1.7). The cavity involved in the model can originate as a result of dislocation interaction following the mechanism described by Fujita (1958).

The models of extrusion and intrusion formation described cannot be treated as a complete explanation. Microcracks are not necessarily preceded by microrelief on the surface. Models introduced below were constructed mostly on the ground of static tests on pure materials, and therefore any conclusions regarding fatigue tests and commercial alloys should be drawn with care.

The hypothesis of Fujita (1958) involves two parallel rows of dissimilar edge